

Performance Regulation and Tracking via Lookahead Simulation: Preliminary Results and Validation

Y. Wardi*, C. Seatzu**, M. Egerstedt*, and I. Buckley*

Abstract—This paper presents an approach to target tracking that is based on a variable-gain integrator and the Newton-Raphson method for finding zeros of a function. Its underscoring idea is the determination of the feedback law by measurements of the system’s output and estimation of its future state via lookahead simulation. The resulting feedback law is generally nonlinear. We first apply the proposed approach to tracking a constant reference by the output of nonlinear memoryless plants. Then we extend it in a number of directions, including the tracking of time-varying reference signals by dynamic, possibly unstable systems. The approach is new hence its analysis is preliminary, and theoretical results are derived for nonlinear memoryless plants and linear dynamic plants. However, the setting for the controller does not require the plant-system to be either linear or stable, and this is verified by simulation of an inverted pendulum tracking a time-varying signal. We also demonstrate results of laboratory experiments of controlling a platoon of mobile robots.

I. INTRODUCTION

Integrative action is an essential element in the steady-state tracking of a constant reference signal by the output of a linear system. However, it is well known that a controller comprised solely of an integrator may have destabilizing effects on the closed-loop system. Therefore tracking controllers often include proportional and derivative elements in addition to an integrator [1], as is standard fare in any undergraduate controls classes. However, purely integrative actions have been used, for example for the regulation of computer processors; Ref. [2] proposed a standalone integral controller endowed with a variable gain in order to enhance the stability margins of the closed-loop system.¹

This idea of a variable gain integrator can be generalized. To illustrate this idea, consider, for example, the single-input-single-output discrete-time system in Figure 1. The objective of the controller is to have the system’s output, $y_n \in R$, with $n = 1, 2, \dots$, denoting time, asymptotically track the given reference $r \in R$. Let $e_n := r - y_n$ denote the error signal, and let $u_n \in R$ be the input signal (control signal) to the plant. The variable gain integrator takes on the form

$$u_n = u_{n-1} + A_n e_{n-1}, \quad (1)$$

*School of Electrical and Computer Engineering, Georgia Institute of Technology, Atlanta, GA 30332. Email: ywardi@ece.gatech.edu, magnus@ece.gatech.edu, ihbuckl@g.clemson.edu.

**Department of Electrical and Electronic Engineering, University of Cagliari, Italy. Email: seatzu@diee.unica.it.

¹These applications include the regulation of power and instruction throughput by the processor’s clock frequency. The rationale behind the choice of such a control architecture, as well as results of simulations on industry benchmark programs, and implementations on Intel’s Haswell microarchitecture [3], can be found in [2], [4], [5].

where $A_n > 0$ is its gain at time n . Note that if $A_n = A \forall n = 1, \dots$, for a given constant A , then the controller acts as an adder, the discrete-time equivalent of an integrator, and hence we call it a variable-gain integrator. Generally A_n is not a constant.

Suppose that the plant is described by a memoryless nonlinearity, $y_n = g(u_n)$ for a continuously-differentiable function $g: R \rightarrow R$. Then A_n can be defined as follows,

$$A_n := \left(\frac{\partial g}{\partial u}(u_{n-1}) \right)^{-1} (r - y_{n-1}), \quad (2)$$

where we assume that the derivative term in Eq. (2) exists and is non-zero.

The resulting tracking (regulation) algorithm consists of a recursive application of Eq. (2), and we note that it comprises an implementation of the Newton-Raphson method for solving the algebraic equation $g(u) = r$. In [2], [4], [5] the use of this variable gain integrator was argued to be competitive with extant techniques for controlling power and instruction-throughput in multicore computer processors despite its simple form. An analysis in a general setting of nonlinear, memoryless systems was carried out in [6].

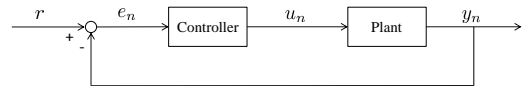


Fig. 1. Basic Control System

The objective of this paper is to extend the aforementioned regulation approach from discrete-time memoryless systems to continuous-time dynamical systems, and from the regulation of constant reference values to the tracking of time-varying reference signals. The extension from discrete-time systems to memoryless continuous-time systems is straightforward and consists of replacing Eq. (2) by a differential equation. However, an extension of the plant from a memoryless system to a dynamical system is more subtle. We propose such an extension by using a nonlinear observer, based on a lookahead simulation of the plant. A key question is how to choose the time-horizon for the lookahead simulation. Large time horizons may yield tracking convergence only for constant reference signals, while the tracking of time-varying signals requires short time horizons. However, short time horizons may render the closed-loop system unstable. To get around this problem we speed up the controller subsystem (but not the plant) which can restore stability thereby yielding tracking convergence.

To our knowledge this approach to tracking is new, and the main objective of the paper is to introduce and explain it, derive preliminary theoretical results, and present results of simulation and laboratory experiments. The general theoretical problem is to classify the systems for which the proposed controller is provably convergent. In such generality the problem is beyond the scope of this paper, but we derive convergence results for memoryless nonlinear plants and dynamic linear plants. Furthermore, we analyze in detail the particular example of position control in systems obeying Newton's second law with a drag. The presented simulation results run ahead of the theoretical developments, and they verify the principles of the tracking technique for various linear and nonlinear systems, with both stable and unstable plants, and with constant target levels as well as time-varying reference signals.

It should be pointed out that the issue of nonlinear regulation is certainly a well-established topic and in this paper we do not provide solutions to problems that were previously not solved. In particular, techniques such as the Byrnes-Isidori regulator [7] based on internal model techniques, or Khalil's high-gain observers for output regulation [8], certainly are more powerful than the methods introduced in this paper. However, the effectiveness of these regulators rely on significant computational sophistication, such as nonlinear inversions and the appropriate nonlinear normal form, e.g., [9], [10]. As such, the contribution in this paper should be understood as a computationally unproblematic, variable gain integrator, and an initial exploration as to when such a structurally simple controller can indeed achieve the desired performance.

In the rest of the paper Section 2 presents the regulation technique with its observer and derives theoretical results, Section 3 provides simulation and experimental verifications, and Section IV concludes the paper.

II. REGULATION AND TRACKING

We start this section by extending the discussion of the system depicted in Figure 1 from discrete time to continuous time. Consider the feedback system shown in Figure 1 except that time $t \geq 0$ is continuous, and hence the signals around the loop are $u(t)$, $y(t)$, and $e(t)$. Suppose that all of these signals are k -dimensional for some $k \geq 1$, and the reference r is a k -dimensional function of time, $r(t) \in \mathbb{R}^k$.

A. Memoryless plant

Consider first the case where the plant is represented by a function $g : \mathbb{R}^k \rightarrow \mathbb{R}^k$, such that for every $t \geq 0$,

$$y(t) = g(u(t)). \quad (3)$$

Suppose also that the function $g(u)$ is continuously differentiable, and that its Jacobian $\frac{\partial g}{\partial u}(u)$ is nonsingular for every $u \in \mathbb{R}^k$ considered in the sequel.

A natural continuous-time equivalent equation to Eqs. (1) and (2) is

$$\dot{u}(t) = \left(\frac{\partial g}{\partial u}(u(t)) \right)^{-1} (r(t) - g(u(t))); \quad (4)$$

here $u(t)$ moves in the direction defined by Newton-Raphson algorithm but the step size is scaled by dt .

Proposition 1: The following limit is in force:

$$\limsup_{t \rightarrow \infty} \|r(t) - y(t)\| \leq \sup \{ \|\dot{r}(t)\| : t \geq 0 \}. \quad (5)$$

Proof: Define $\rho := \sup \{ \|\dot{r}(t)\| : t \geq 0 \}$. Define the function $V : \mathbb{R}^k \times \mathbb{R}^+ \rightarrow \mathbb{R}^+$ by

$$V(u, t) = \frac{1}{2} \|r(t) - y(t)\|^2. \quad (6)$$

Taking derivatives with respect to t , and by Eqs. (3) and (4),

$$\dot{V}(u(t), t) = (r(t) - y(t))^T (\dot{r}(t) - (r(t) - y(t))). \quad (7)$$

Fix $\varepsilon \in (0, 1)$. By Eq. (7), if $\|r(t) - y(t)\| > (1 + \varepsilon)\rho$, then

$$\dot{V}(u(t), t) \leq -\varepsilon(1 + \varepsilon)\rho^2. \quad (8)$$

By Lyapunov direct method [11] it follows that $\limsup_{t \rightarrow \infty} \|r(t) - y(t)\| \leq (1 + \varepsilon)\rho$, and since $\varepsilon > 0$ can be arbitrarily small, Eq. (5) is satisfied. ■

Remarks: 1). In the special case where $r(t) = r \in \mathbb{R}^k$, a constant, the function $V(u) := V(u, t)$ is a Lyapunov function, and it follows that, as $t \rightarrow \infty$, $\lim y(t) = r$.

2). Proposition 1 means that asymptotically $y(t)$ is confined to a ball with center $r(t)$ and radius ρ . To reduce this radius we can increase the controller's gain by multiplying the RHS of (4) by $\alpha > 1$. The control equation then becomes

$$\dot{u}(t) = \alpha \left(\frac{\partial g}{\partial u}(u(t)) \right)^{-1} (r(t) - g(u(t))). \quad (9)$$

With the Lyapunov function $V(u, t)$ defined by (6), the same arguments comprising the proof of Proposition 1 yield that

$$\limsup_{t \rightarrow \infty} \|r(t) - y(t)\| \leq \frac{1}{\alpha} \sup \{ \|\dot{r}(t)\| : t \geq 0 \}. \quad (10)$$

We next extend this tracking control law to dynamic plants.

B. The plant as a dynamical system

Suppose that the plant is represented by a differential equation of the form

$$\dot{x}(t) = f(x(t), u(t)), \quad t \geq 0, \quad (11)$$

where $x(t) \in \mathbb{R}^n$, for a function $f : \mathbb{R}^n \times \mathbb{R}^k \rightarrow \mathbb{R}^n$; the initial state is $x_0 := x(0)$. The output $y(t)$ is given by

$$y(t) = h(x(t)) \quad (12)$$

for a function $h : \mathbb{R}^n \rightarrow \mathbb{R}^k$.

The following assumption ensures that the state variable $x(t)$ and the output $y(t)$ are well defined for all $t \geq 0$.

Assumption 1: 1). For every $u \in \mathbb{R}^k$, the function $f(x, u)$ is continuously-differentiable in x , and the functions $f(x, u)$ and $\frac{\partial f}{\partial u}(x, u)$ are locally Lipschitz continuous in (x, u) . 2). The function $h(x)$ is continuously differentiable in x . 3). For every compact set $U \subset \mathbb{R}^k$ there exist $K_1 > 0$ and $K_2 > 0$ such that, for every $(x, u) \in \mathbb{R}^n \times U$, $\|f(x, u)\| \leq K_1 \|x\| + K_2$.

In extending the control law from the memoryless case (Eq. (4)) to the dynamic-plant case it is necessary to first

define the function $g(u)$, and there is no single natural way to do it. Our choice of $g(u)$ is based on an evaluation of the system's output T seconds in the future by a lookahead simulation for a given $T > 0$. Specifically, suppose that at time t the state $x(t)$ is measured, and a lookahead simulator computes what the output would be at time $t+T$ if the input were $u(\tau) = u(t) \forall \tau \in [t, t+T]$. The result of this computation is $g(u)$. Formally, given $t \geq 0$, $x \in \mathbb{R}^n$, $u \in \mathbb{R}^k$ and $T > 0$, let $\xi(\tau) \in \mathbb{R}^n$ be defined by the equation

$$\dot{\xi}(\tau) = f(\xi(\tau), u) \quad (13)$$

with the boundary condition $\xi(t) = x$; note that the input is a constant $u(\tau) = u \forall \tau \in [t, t+T]$. We use the notation $\phi(x, t; u, \tau) = \xi(\tau)$ to emphasize its dependence on x , t and $\tau \geq t$ in addition to u . In a specific run of the system, let $x(t)$ denote its state variable at time t so that its output is $y(t) = h(x(t))$ according to Eq. (12). Suppose also that at time t , $x(t)$ can be measured and a lookahead simulation can compute $\phi(x(t), t; u(t), t+T)$; note that in this simulation the input to the plant-model in the simulator is $u(t) \forall \tau \in [t, t+T]$. Then $g(u)$ is defined as follows,

$$g(u) = h(\phi(x(t), t; u(t), t+T)). \quad (14)$$

Of course $g(u)$ is a function of t , $x(t)$ and T in addition of u , but we use the simplified notation $g(u)$ when no confusion arises.

The feedback law is defined by adjusting Eq. (4) to the present case of dynamic plants. The only difference is to replace $r(t)$ in (4) by $r(t+T)$, resulting in the equation

$$\dot{u}(t) = \left(\frac{\partial g}{\partial u}(u(t)) \right)^{-1} (r(t+T) - g(u(t))). \quad (15)$$

The reason for this change is that Eq. (4) is designed to match $g(u(t))$ to $r(t)$, whereas in Eq. (15) $g(u)$ is an estimator of $y(t+T)$ and hence it is designed to match $r(t+T)$.

The closed-loop system is comprised of the plant and the controller subsystems, defined by Eqs. (11) and (15), respectively. The computation of (15) including its various ingredients, $g(u(t))$ and $\frac{\partial g}{\partial u}(u(t))$, can be performed by any numerical technique for differential equations; we use the forward-Euler method in all examples described in the sequel.

Thus far the discussion of Eq. (15) has been predicated on its exact computation. However, in practical situations one can expect errors due to several factors, including measurements of $x(t)$, modelling uncertainties, and computational errors. An error analysis cannot fit in the paper due to its space limitation and hence will be presented in a forthcoming publication. We anticipate a result similar to Eq. (5) where $\dot{r}(t)$ is replaced by a cumulative measure of the various errors.

An extension of Proposition 1 to the present setting of dynamical systems does not work for the following two reasons: First, the closed-loop system may be unstable, while this is not a problem for memoryless plants as can be seen in the proof of Proposition 1. Second, such a result, if true, would imply the tracking of $r(t+T)$ by $g(u)$ which is not the

same as $y(t+T)$. Generally the error term $\|g(u) - y(t+T)\|$ can be made small by choosing a small $T > 0$. However, we shall see that often the closed-loop system is stable for large T and unstable for small T . One approach to this difficulty is to choose a small T and then try to stabilize the system by scaling up the Right-Hand Side (RHS) of Eq. (15). This is not the same as increasing the controller's gain (unless the plant system is memoryless) and may have a stabilizing effect on the closed-loop system. We shall see that for a particular class of Linear, Time-Invariant (LTI) systems, for a given value of $T > 0$, the tracking of a constant reference $r \in \mathbb{R}^k$ is achieved as long as the closed-loop system is stable.

The derivation of sufficient conditions for tracking for general nonlinear systems is beyond the scope of this paper. Instead, we next derive some theoretical results only for linear systems, but later provide simulation results for linear and nonlinear systems.

C. The plant as an LTI system

Consider the case where the plant has the form

$$\dot{x}(t) = Ax(t) + Bu(t), \quad y(t) = Cx(t), \quad (16)$$

where the matrix-dimensions are $A \in \mathbb{R}^{n \times n}$, $B \in \mathbb{R}^{n \times k}$, $C \in \mathbb{R}^{k \times n}$. Suppose that A is nonsingular. Fix $T > 0$, and suppose that the matrix $(CA^{-1}(e^{AT} - I_n)B)$ is nonsingular as well, where I_n denotes the $n \times n$ identity matrix. By solving the differentiable equation (13), and by Eq. (14), it is readily seen that

$$g(u) = C \left(e^{AT} x(t) + A^{-1}(e^{AT} - I_n)Bu \right), \quad (17)$$

and hence

$$\frac{\partial g}{\partial u}(u) = CA^{-1}(e^{AT} - I_n)B. \quad (18)$$

By Eq. (15), after some algebra it follows that

$$\dot{u}(t) = \left(CA^{-1}(e^{AT} - I_n)B \right)^{-1} (r(t+T) - Ce^{AT}x(t)) - u. \quad (19)$$

Define the $(n+k) \times (n+k)$ matrix Φ_T by

$$\Phi_T = \begin{pmatrix} A & B \\ -\left(CA^{-1}(e^{AT} - I_n)B \right)^{-1} Ce^{AT} & -I_k \end{pmatrix}, \quad (20)$$

where I_k is the $k \times k$ identity matrix, and define the $k \times k$ matrix Ψ_T by

$$\Psi_T = \left(CA^{-1}(e^{AT} - I_n)B \right)^{-1}. \quad (21)$$

Then the closed-loop system comprised of Eqs. (16) and (19) has the form

$$\begin{pmatrix} \dot{x}(t) \\ \dot{u}(t) \end{pmatrix} = \Phi_T \begin{pmatrix} x(t) \\ u(t) \end{pmatrix} + \begin{pmatrix} 0 \\ \Psi_T \end{pmatrix} r(t+T). \quad (22)$$

Lemma 1: Suppose that A is Hurwitz. There exists $\bar{T} > 0$ such that for every $T \geq \bar{T}$, the matrix Φ_T is Hurwitz.

Proof: By assumption, $\lim_{T \rightarrow \infty} e^{AT} = 0$. Therefore, and by (20),

$$\lim_{T \rightarrow \infty} \Phi_T = \begin{pmatrix} A & B \\ 0 & -I_k \end{pmatrix}. \quad (23)$$

By assumption, this matrix is Hurwitz. \blacksquare

The next result concerns the tracking of a constant reference $r \in R^k$ by the output of an LTI system. Given $r \in R^k$. Fix $T > 0$, and assume that A is nonsingular.

Lemma 2: Suppose that Φ_T is Hurwitz. Then

$$\lim_{t \rightarrow \infty} y(t) = r. \quad (24)$$

Proof: By Eq. (22) with $r(t+T) \equiv r$, and the assumption that Φ_T is Hurwitz, the state variable $x(t)$ and the input $u(t)$ have asymptotic values, namely, there exist $x \in R^n$ and $u \in R^k$ such that, $\lim_{t \rightarrow \infty} x(t) = x$ and $\lim_{t \rightarrow \infty} u(t) = u$. Correspondingly, $\lim_{t \rightarrow \infty} \dot{x}(t) = 0$ and $\lim_{t \rightarrow \infty} \dot{u}(t) = 0$. Furthermore, by the second part of Eq. (16), $\lim_{t \rightarrow \infty} y(t) = cx$.

Taking the limit $t \rightarrow \infty$, by (16), $Ax + Bu = 0$. By (19) with $r(t+T) \equiv r$, $r - Ce^{AT}x - CA^{-1}(e^{AT} - I_n)Bu = 0$, and since $Ax + Bu = 0$, we have that

$$r - Ce^{AT}x + CA^{-1}(e^{AT} - I_n)Ax = 0. \quad (25)$$

This implies, after some algebra, that $r - Cx = 0$, hence Eq. (24) is satisfied. \blacksquare

As a corollary of Lemma 1 and Lemma 2, if A is Hurwitz then there exists $\bar{T} > 0$ such that, with every $T \geq \bar{T}$, the system will track any given constant $r \in R^k$.

D. Example

Consider the problem of controlling the position of a particle by the force applied to it. The model we use is a second-order system with a drag, obeying Newton's second law. Thus, denoting by $y \in R$ the position of a particle with respect to a given reference, let $v \in R$ denote its velocity, and let $u \in R$ be the applied force. The motion equations are $\dot{y}(t) = v(t)$ and $\dot{v}(t) = av(t) + u(t)$, for given initial conditions $y_0 := y(0)$ and $v_0 := v(0)$, where $a \in R$ is the drag coefficient. In a physical system $a < 0$, but we allow for $a > 0$ in order to extend the discussion to unstable systems. However, we assume henceforth that $a \neq 0$ since the case where $a = 0$ requires a different set of equations than those derived in the sequel. Given $r > 0$, the objective is to regulate $y(t)$ to rt , namely to achieve the limit $\lim_{t \rightarrow \infty} (y(t) - rt) = 0$.

Defining the state variables by $x_1(t) = y(t) - rt$ and $x_2(t) = v(t)$, the state equation is

$$\begin{aligned} \dot{x}_1(t) &= x_2(t) - r \\ \dot{x}_2(t) &= ax_2(t) + u(t), \end{aligned} \quad (26)$$

with initial conditions $x_{1,0} := x_1(0)$ and $x_{2,0} := x_2(0)$. The objective is to control $x_1(t)$ in the sense that

$$\lim_{t \rightarrow \infty} x_1(t) = 0. \quad (27)$$

By Eq. (13), and solving analytically the state equation (26), it is readily seen that

$$g(u(t)) = x_1(t) + \frac{1}{a}(e^{at} - 1)x_2(t) + \frac{1}{a^2}(e^{at} - 1)u - \frac{T}{a}u - rT, \quad (28)$$

and hence

$$\frac{\partial g}{\partial u}(u) = \frac{1}{a^2}(e^{at} - 1) - \frac{T}{a}. \quad (29)$$

Considering Eqs. (15), (26) with $r(t+T) \equiv 0$, and applying Eqs. (14), (28), (29), and (22) we obtain, after some algebra, that

$$\Phi_T = \begin{pmatrix} 0 & 1 & 0 \\ 0 & a & 1 \\ -\frac{a^2}{e^{aT} - 1 - aT} & -\frac{a(e^{aT} - 1)}{e^{aT} - 1 - aT} & -1 \end{pmatrix}; \quad (30)$$

the matrix Ψ_T in (22) is irrelevant to the present discussion. The characteristic polynomial of Φ_T is

$$\begin{aligned} \chi(\lambda) &= \lambda^3 + (1-a)\lambda^2 \\ &+ \frac{a^2T}{e^{aT} - 1 - aT}\lambda + \frac{a^2}{e^{aT} - 1 - aT}. \end{aligned} \quad (31)$$

Lemma 2 ensures that tracking, in the sense of Eq. (27), is achieved if Φ_T is Hurwitz.

Proposition 2: The matrix Φ_T is Hurwitz if and only if the following two conditions are satisfied: (i) $a < 1$, and (ii) $T > \frac{1}{1-a}$.

Proof: Consider the Routh test. Denote the entries of the first column in the Routh table by c_i , $i = 3, 2, 1, 0$, in decreasing order. Then $c_3 = 1$, $c_2 = 1 - a$, $c_1 = \frac{(1-a)a^2T - a^2}{(e^{aT} - 1 - aT)(1-a)}$, and $c_0 = \frac{a^2}{e^{aT} - 1 - aT}$. Now $c_3 > 0$, while $c_2 > 0$ if and only if $a < 1$. Next, for every $x \neq 0$, $e^x - 1 - x > 0$, this follows from the facts that, with the function $\zeta(x) := e^x - 1 - x$, $\zeta'(x) > 0$ for $x > 0$, $\zeta'(x) < 0$ for $x < 0$, and $\zeta(0) = 0$. This implies that $c_0 > 0$. Φ_T is Hurwitz if and only if $a < 1$ and $c_1 > 0$. For $a < 1$, it is readily seen that $c_1 > 0$ if and only if $T > \frac{1}{1-a}$. \blacksquare

Note that for $a > 1$ no $T > 0$ will yield tracking. On the other hand, for $a \in (0, 1)$, tracking is attained as long as $T > \frac{1}{1-a}$ even though the plant is unstable.

We mention that for $a > 1$ it is possible to scale up the RHS of Eq. (15) in order to guarantee tracking. Multiplying the RHS of Eq. (15) by $\alpha > 1$ results in the scaling of the last row of the matrix Φ_T in (30) by α . A bit of algebra reveals that the entries in the first column of the Routh table are $c_3 = 1$, $c_2 = \alpha - a$, $c_1 = \frac{(\alpha-a)a^2T - a^2\alpha}{(e^{aT} - 1 - aT)(\alpha-a)}$, and $c_0 = \frac{\alpha a^2}{e^{aT} - 1 - aT}$. The arguments in the proof of Proposition 2 yield that tracking is attained if and only if $a < \alpha$ and $T > \frac{1}{\alpha-a}$. All of this will be demonstrated by simulation in the next section.

III. SIMULATION AND LABORATORY EXPERIMENTS

This section presents simulation results on three systems: the position-control system described in the last section, an inverted pendulum, and a platoon of mobile robots. For the first system we consider the tracking of a ramp where we verify the theoretical results derived in Section II.D, then we consider an unstable system tracking a sinusoid. The inverted pendulum provides an example of a nonlinear, unstable system tracking a sinusoid, and in the platoon example we control the interspacing between successive vehicles. The first two systems are simulated by MATLAB codes for solving their respective state equations via Euler's forward method with integration step sizes of $dt = 0.01$. In contrast, the platoon system is implemented in a laboratory setting. In all three cases the lookahead simulation for computing $g(u)$

and $\frac{\partial g}{\partial u}(u)$, hence the control law, involves the Forward Euler method with integration step sizes of $\Delta t := 0.01T$.

A. Position-control system

Consider the system described in Section II.D, where the objective is to have the position $y(t)$ track a ramp rt for $r = 2$. The system is defined by Eq. (26), and the objective is to attain Eq. (27). The controller is defined by (15), and by Lemma 2, tracking is attained as long as the matrix Φ_T is Hurwitz. By Proposition 2, this is the case if and only if $a < 1$ and $T > \frac{1}{1-a}$. We next verify this conclusion.

Let $a = -1$ so that the plant system is stable, and let $T = 1$ which ensures that the closed-loop system is stable. Following a simulation of the system, the graph of $x_1(t)$ vs. t is depicted in Figure 2 by the solid graph, and it indicates tracking. Next we change T to $T = 0.5$, which is on the boundary of the stability region. The resulting graph of $x_1(t)$, shown by the dashed graph in Figure 2, indicates growing oscillations and hence instability. Theoretically one may expect undamped oscillations at $T = 0.5$ because the closed-loop system is marginally stable, but that is obtained for a slightly larger T , namely $T = 0.53$ (results not shown). The discrepancy is due to the use of the forward Euler integration which can destabilize marginally-stable systems. Several experiments with various values of $T < 0.53$, not shown here, resulted in instability of the closed-loop system.

For the next experiment we make two changes to the system: a is set to $a = 0.5$ hence the plant system is unstable, and the tracking's target is a time-varying signal $r(t) := 2 + \sin t$. Due to the value of a , stability of the closed-loop system requires that $T > 2$. First we take $T = 3$ to ensure stability. The resulting graph of the position $y(t)$ is depicted by the dashed curve in Figure 3, and for the sake of reference we plotted $r(t)$ by the dot-dashed curve.² We notice stability of the closed-loop system but no tracking; larger simulation horizons do not change this conclusion. It is not surprising in light of the discussion in Section II, since T is too large for $g(u)$ to yield an adequate approximation for $y(t + T)$. Therefore we reduce T to $T = 0.4$ in order to get a better approximation. However, this value is not in the stability range. Therefore we speed up the controller by multiplying the RHS of Eq. (15) by $\alpha = 5.0$. The resulting graph of $y(t)$ is depicted by the solid curve in Figure 3, and we see there stability and as well as tracking. It must be pointed out that in the first 3 seconds the motion may experience a large jerk. This issue can be addressed by ad-hoc methods like gradual increases of the gain α , which are beyond the scope of this paper but will be considered in the near future.

²Actually the dot-dashed curve looks like a solid curve after the first half-cycle of the sinusoid since it is merged there with another graph (described below). The dot-dashed part of the sinusoid is visible during its first half-cycle.

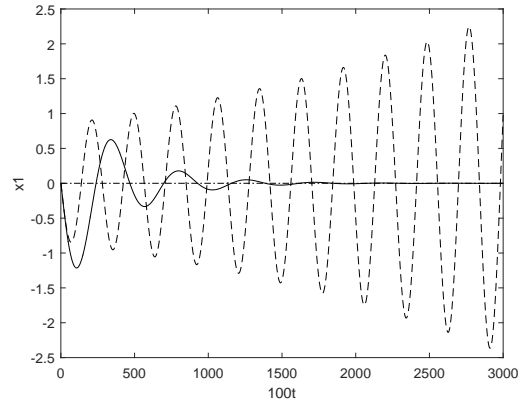


Fig. 2. Position-control system: constant target

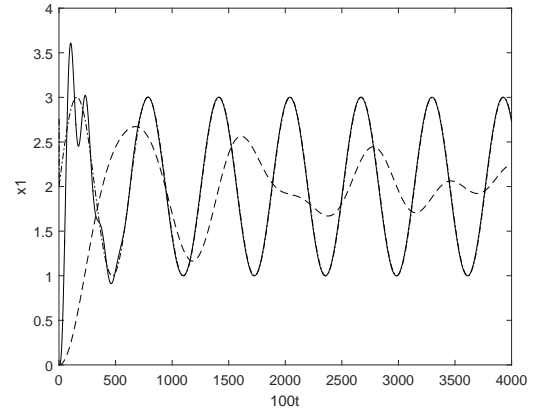


Fig. 3. Position control system: sinusoidal target

B. Inverted pendulum

The equations for the inverted-pendulum that we use are

$$\begin{aligned} \dot{x}_1(t) &= x_2(t) \\ \dot{x}_2(t) &= a \sin x_1 - bx_2 + u(t), \end{aligned} \quad (32)$$

where x_1 is the angle of the pendulum from the upper equilibrium point and x_2 is its angular velocity; $a > 0$ and $b > 0$ are given positive constants. We chose (arbitrarily) $a = 1.0$ and $b = 0.2$. In the first experiment we regulate the angle x_1 to the target $\pi/6$. We set the lookahead parameter T first to $T = 2.0$ and then to $T = 0.8$. The results are shown in Figure 4, where the dotted horizontal line indicates the target level of $\pi/6$. For $T = 2$, the graph of the angle $x_1(t)$ is depicted by the solid curve, and we discern stability and tracking. However, for the smaller value of $T = 0.8$, the graph of x_1 , depicted by the dashed curve, indicates that the closed-loop system is unstable and no tracking is achieved. These results are consistent with the discussion in Section II suggesting that stability of the closed-loop system is more likely to be attained for larger values of T .

Consider next the tracking of the curve $r(t) = \frac{\pi}{6} + \frac{\pi}{8} \sin t$. For $T = 2.0$, the results are shown in Figure 5, where the dash-dotted curve depicts the graph of $r(t)$, and the dashed

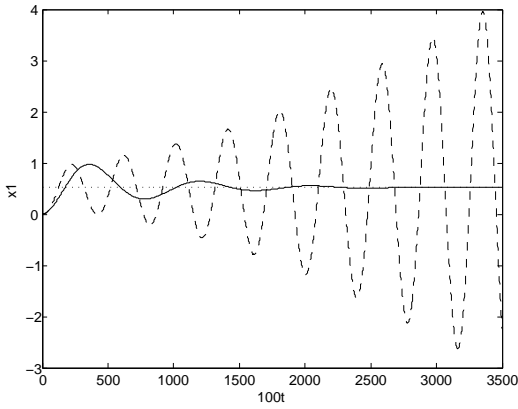


Fig. 4. Inverted pendulum: constant target

graph is of $x_1(t)$.³ It is evident that the closed-loop system is stable but no tracking is achieved. We then set T to $T = 0.15$, but the resulting closed-loop system is unstable; in fact, the oscillations in $x_1(t)$ (not shown in the figure) reach a magnitude of about 10^{21} at $t = 35$. To address this problem we speed up the controller by multiplying the RHS of (15) by $\alpha = 20$. The resulting graph of $x_1(t)$ is depicted in Figure 5 by the solid curve, and it is evident that tracking has been attained. We point out that the parameter-values $T = 0.15$ and $\alpha = 20$ were chosen after some trial and error, but during that process it was quite evident that smaller T yields better tracking but requires larger α . For instance, increasing T from $T = 0.15$ to $T = 0.2$, $\alpha = 8$ sufficed to give tracking and the graph of $x_1(t)$ was quite similar to that shown in Figure 5. Judging by the error $\mathcal{E} := \int_5^{35} |r(t) - x_1(t)| dt$, for $T = 0.15$ and $\alpha = 20$, $\mathcal{E} = 1.056$; while for $T = 0.2$ and $\alpha = 8$, $\mathcal{E} = 1.419$. These errors correspond to average errors $|x_1(t) - r(t)|$ over $t \in [5, 35]$ of 0.035 and 0.047, respectively.

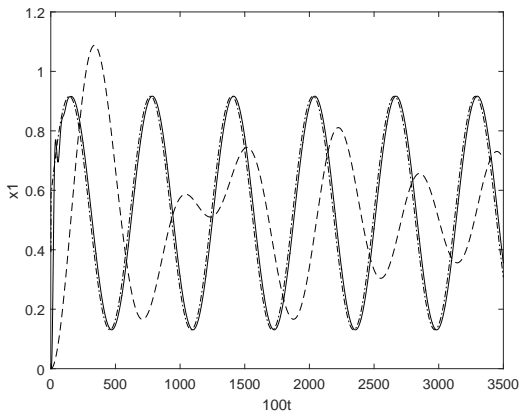


Fig. 5. Inverted pendulum: sinusoidal target

C. Platoon of mobile robots

Consider a platoon of mobile robots (vehicles) tasked with sequentially following a given path in R^2 in a predetermined

³It may be hard to distinguish the dash-dotted curve from a solid curve with which it is almost aligned. The solid curve will be explained shortly.

order. Denote by R_i , $i = 1, \dots, N$ the robots in their sequential order. The vehicles are autonomous in the sense that each one of them controls its own motion. The objective is to have the first (leading) robot, R_1 , regulate its speed to a given reference, and for every $i = 2, \dots, N$, R_i , is to regulate its distance to R_{i-1} . This problem has been extensively investigated in the context of automated highway and urban traffic control, and recently an interest in it has sprouted in the setting of smart cities; see. e.g., [12], [13] for surveys.

The experiments described below were run in a swarm robotic testbed laboratory, the *Robotarium*, situated in the Georgia Tech campus [14]. The robots, GRITsbots [15], and their motion can be controlled directly by their velocities via differential-drive motors. The differential drive robots are modelled by unicycle dynamics. Following [16], rather than directly specifying the translational and angular velocities of each robot, we instead control a point-particle in the front of each robot with the simple dynamics,

$$\dot{x}_i = u_i, \quad (33)$$

and map this onto the dynamics of the robot.

The subject of the experiment is a platoon of eight robots, and the goal is to have them move counter-clockwise on a given reference circle at a predetermined speed while maintaining a given interspacing of d cm between R_i and R_{i-1} . The center and radius of the reference circle are given $C \in R^2$ and $r > 0$, hence it is denoted by $B(C, r)$. The first robot, R_1 , starts on $B(C, r)$ and is programmed to stay on it while controlling its velocity to the given target. Each subsequent robot R_i , $i = 2, \dots, N$, attempts, at time t , to regulate its position to the point of (Euclidean) distance d behind R_{i-1} on the circle $B(C, r)$. The parameters for the experiments are as follows: $r = 28$ cm and $d = 14$ cm, the robot's dimension is 3 cm \times 3 cm, and the point which is controlled is 3 cm ahead of the robot. The lookahead parameter for the controller (Eq. (15)) is $T = 0.6$ s, and the scaling factor of the RHS of (15) is $\alpha = 45$.

The results of the experiments can be seen in the video clip [17], where we see that although all the robots start close to the circle $B(C, r)$, some of their trajectories initially move away from it and display an erratic behaviour. However, they soon turn to the circle and track their target distance from each other. Figure 6 displays the progress of the tracking assignments by providing snapshots of the robots' locations at times $t = 0$, $t = 7$ s (200 iterations), and $t = 20$ s (600 iterations). Finally, Figure 7 depicts the graphs of the distance between adjacent robots, $\|x_i - x_{i-1}\|$, with roughly 30 iterations per second, and we see that the interspace tracking has been achieved.

IV. CONCLUSIONS

This paper proposes a technique for performance regulation and tracking of dynamical systems via lookahead simulation. It is based on steering the control signal in a

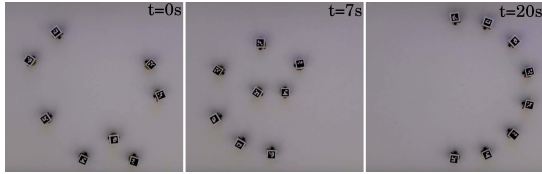


Fig. 6. Positions of robots at times at times 0 (left), 7s (center), and 20s (right)

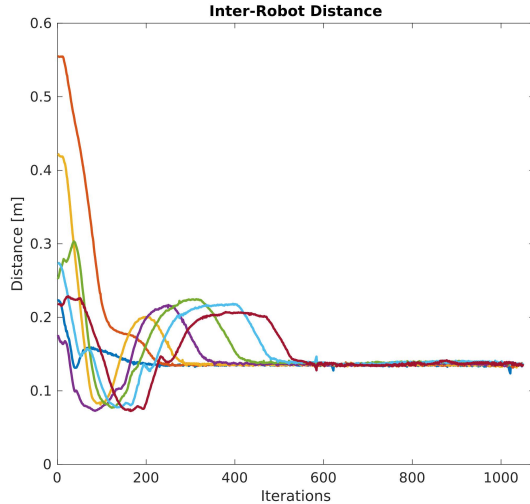


Fig. 7. Interspending between adjacent robots

direction determined by the Newton-Raphson method for solving an algebraic equation, the loop equation. The resulting controller can be nonlinear. Preliminary theoretical results are derived for memoryless nonlinear systems and dynamic linear systems. Simulation experiments support the theoretical developments, and go beyond them to include nonlinear dynamical systems such as the inverted pendulum. A laboratory experiment of interspending control in a platoon of mobile robots is described as well.

A key question concerns the determination of the lookahead timing parameter T for the simulations defining the controller. The derived theoretical and simulation results indicate that stability of the closed-loop system may require large T , while tracking may require small T . This tradeoff has been resolved for the systems under study by first picking a small T , then stabilizing the system (if needed) by speeding up the action of the controller. Identifying the kind of systems for which this regulation and tracking technique works constitutes a subject of future research.

REFERENCES

- [1] G.F. Franklin, J.D. Powell, and A. Emami-Naeini. *Feedback Control of Dynamic Systems*, Prentice Hall, Pearson, 2014.
- [2] N. Almoosa, W. Song, Y. Wardi, and S. Yalamanchili. A Power Capping Controller for Multicore Processors. *Proc. 2012 American Control Conference*, Montreal, Canada, June 27-29, 2012.
- [3] P. Hammarlund, A.J. Martinez, A.A. Bajwa, D.L. Hill, E. Hallnor, H. Jiang, M. Dixon, M. Derr, M. Hunsaker, R. Kumar, R.B. Osborne, R. Rajwar, R. Singhal, R. D'Sa, R. Chappell, S. Kaushik, S. Chennupati, S. Jourdan, S. Gunther, T. Piazza, and T. Butron. Haswell: The Fourth-Generation Intel Core Processor. *IEEE Micro*, Vol. 34, Issue 2, pp. 6 - 20, 2014.

- [4] X. Chen, H. Xiao, Y. Wardi, and S. Yalamanchili. Throughput Regulation in Shared Memory Multicore Processors. *Proc. 22nd IEEE Intl. Conference on High Performance Computing (HiPC)*, Bengaluru, India, December 16-19.
- [5] X. Chen, Y. Wardi, and S. Yalamanchili. IPA in the Loop: Control Design for Throughput Regulation in Computer Processors. *Proc. 13th Intl. Workshop on Discrete Event Systems (WODES 16)*, Xi'an, China, May 30 to June 1.
- [6] Y. Wardi, C. Seatzu, X. Chen, and S. Yalamanchili. Performance Regulation of Event-Driven Dynamical Systems Using Infinitesimal Perturbation Analysis. *Nonlinear Analysis: Hybrid Systems*, Volume 22, pp. 116-136, November 2016.
- [7] A. Isidori and C.I. Byrnes. Output regulation of nonlinear systems. *IEEE Transactions on Automatic Control*, Vol. 35, pp. 131-140, 1990.
- [8] H.K. Khalil. On the design of robust servomechanisms for minimum phase nonlinear systems. *Proceedings of the 37th IEEE Conference on Decision and Control*. Tampa, FL. pp. 3075-3080, 1998.
- [9] A. Isidori. *Nonlinear Control Systems, Third Ed.* Springer-Verlag, Berlin, 1995.
- [10] S. Sastry. *Nonlinear Systems: Analysis, Stability, and Control*. Springer Verlag, 1999.
- [11] H.K. Khalil. *Nonlinear Systems, Third Ed.* Prentice Hall, 2002.
- [12] T. Hunter, T. Das, M. Zaharia, P. Abbeel, and A. Bayen. Large Scale Estimation in Cyberphysical Systems Using Streaming Data: A Case Study With Arterial Traffic Estimation. *IEEE Transactions on Automation Science and Engineering*, Vol. 10, No. 3, pp. 884-898, Oct. 2013.
- [13] C.G. Cassandras. Smart Cities as Cyber-Physical Social Systems. *Engineering*, Vol. 2, No. 2, pp. 156-158, June 2016.
- [14] D. Pickem, P. Glotfelter, L. Wang, M. Mote, A. Ames, E. Feron, and M. Egerstedt. The Robotarium: A Remotely Accessible Swarm Robotics Research Testbed. To appear, *Proc. IEEE International Conference on Robotics and Automation*, 2017.
- [15] D. Pickem, M. Lee, and M. Egerstedt. The GRITSBot in its natural habitat-a multi-robot testbed. *Proc. IEEE Intl. Conf. Robotics and Automation (ICRA)*, pp. 4062-4067, 2015.
- [16] R. Olfati-Saber. Near-identity diffeomorphisms and exponential epsilon-tracking and epsilon-stabilization of first-order nonholonomic $se(2)$ vehicles. *Proc. American Control Conference*, 2002.
- [17] I.H. Buckley. <https://youtu.be/GdVsbroDCeE> or <http://gritlab.gatech.edu/home/2017/03/performance-regulation-and-tracking-via-lookahead-simulation-preliminary-results-and-validation/> March 2017.